Bioprocess Engineering 1 (1986) 3–11

Bioprocess Engineering

Stability analysis of a binary culture chemostat experiencing biofilm formation

J. D. Bryers, Durham, NC, USA

Abstract. Time-dependent biofilm formation effects on continuous fermenter operation are modelled here for a binary culture of microorganisms growing on a single substrate. Dynamic computer solutions are detailed for a mixed culture of one microbe a having a higher growth rate than a second microbe b for two hypothetical scenarios of microbe b having different magnitudes of cellular deposition rate. A stability analysis of the resultant steady-states is also provided. Biofilm effects on the estimation of kinetic and stoichiometric parameters in a chemostat plus the impact of biofilms on mixed culture dynamics are discussed.

1 Introduction

Based upon accepted material balances and quantitative mathematical descriptions of microbial growth processes, models have been derived which can simulate a variety of indirect interactions (e.g., commensalism, mutualism, product or substrate inhibition, etc.) within mixed cultures of microorganisms. A general set of equations for a dual microorganism culture, microbe a and b, competing in a chemostat for p possible growth limiting substrates, producing q possible metabolic products, and v secondary substrates, can be written as follows:

$$dC_a/dt = -DC_a + \mu_a C_a, \tag{1}$$

$$dC_b/dt = -DC_b + \mu_b C_b, \tag{2}$$

$$dS_i/dt = D(S_i^0 - S_i) - \mu_a C_a/Y_a - \mu_b C_b/Y_b, \quad \text{where } i = 1 \to p, \tag{3}$$

$$dr_j/dt = -Dr_j + \alpha_{a,j}\mu_a C_a + \alpha_{b,j}\mu_b C_b, \quad \text{where } j = 1 \to q, \tag{4}$$

$$du_k/dt = -Du_k + \beta_{a,k}\mu_a C_a + \beta_{b,k}\mu_b C_b, \quad \text{where } k = 1 \to v, \tag{5}$$

where C_a is the concentration of microbe a, C_b is the concentration of microbe b, S_i is the concentration of limiting substrates $i = 1 \to p$, r_j is the concentration of secondary metabolites (considered inhibitory) $j = 1 \to q$, u_k is the concentration of secondary products serving as potential substrates $k = 1 \to v$, D is the dilution rate, $\mu_{a,b}$ are the growth rates of microbes a and b, respectively, on the various possible substrates, $\alpha_{a,j}$ and $\alpha_{b,j}$ are the stoichiometric coefficients for secondary metabolite production, and $\beta_{a,k}$ and $\beta_{b,k}$ are the stoichiometric coefficients for secondary substrate production. Selection of the functional form of μ_a and μ_b depends upon the system under consideration. Consequently, Eqs. (1)–(5) can provide, with appropriate selected rate expressions, a general framework for all possible cases of mixed culture interactions.

Dynamic behavior of special cases of Eqs. (1)–(5) has received much attention in recent years [1–5]. Stability analysis of continuous mixed culture reactors allows for (1) qualitative criteria for model validity testing and (2) quantitative assessment of reactor performance. The technique most frequently used in determining the stability of the steady states of such systems is based upon Lyapunov's first method [6]. Effectively, the system differential equations are linearized about a steady-state of interest, and the eigenvalues of the resultant Jacobian matrix evaluated. However, frequently, the above stability analysis fails to relate to actual situations. Commonly, there are several system factors that act as stability enhancers which are not considered in the ideal situation. Among such realities are (a) more complex interconnected interaction schemes (i.e., competition and mutualism or competition and inhibition) and (b) temporal and/or spatial inhomogeneities (e.g., multistage systems, biofilm formation, incomplete mixing).

This paper will consider the effect of biofilm formation on the mixed culture dynamics in a chemostat. First, a simple model for biofilm formation in a binary culture chemostat is derived. Then, the binary culture of one microbe (C_a) having a higher growth rate than a second microbe (C_b) is considered for two hypothetical scenarios of microbe b having two different magnitudes of cell-surface attachment rate. Stability analysis of the simple biofilm model is considered for several pertinent steady state situations. Finally, the behavior of a chemostat

experiencing biofilm formation is discussed with regard to data interpretation and resultant ecological conclusions.

2 Biofilm formation in fermenters

Biofilms, adherent microorganisms often entrapped within an extracellular polymeric matrix, can develop on any surface exposed to an active microbial culture. Biofilms within fermenters can create such problems as: 1) erratic effluent biomass concentrations, 2) an obscure continuous culture wash-out, 3) atypical ecological niches within the reactor, and 4) physical fouling of reactor internals (e.g., impellers, baffles, heat exchangers, pH and DO probes). Despite an increasing awareness of biofilm formation in various systems and the associated detrimental effects [7], biofilm formation in a chemostat is often only considered a mere operating nuisance. Interpretation of resultant chemostat data all to often ignores the subtle effects of biofilms; such neglect can produce inaccurate estimates of kinetic/stoichiometric parameters and can lead to erroneous conclusions about ecological dynamics of mixed cultures. Historically, the effects of biofilm formation on fermenter operation were not considered until 1964 [8, 9] even though the effects of microbial attachment on microbial activity were noted in 1943 [10]. Topiwala and Hamer [11] first quantified the effects of a constant biofilm amount on the steady-state substrate and suspended biomass concentrations in a chemostat. This classical note predicted the extension (or elimination) of culture wash-out as a function of the assumed constant biofilm amount. The Topiwala-Hamer model (THM) was derived for pure cultures with constant kinetic/stoichiometric parameters equal for both attached and suspended microorganisms; no mass transfer limitations were considered. Wilkinson and Hamer [12] experimentally verified the THM in continuous mixed culture studies where the biofilm was reported at $\approx 700\,\mu m$. Biofilm research increased dramatically during the seventies with most theoretical efforts directed toward modelling substrate mass transfer and biological reaction within a biofilm of constant thickness. Grady [13] provides an excellent review of such biofilm kinetic models. Characklis and colleagues [7, 14–16] present the only comprehensive studies (both experimental and theoretical) of biofilm accumulation in continuous well-mixed reactors; unfortunately in their work, biofilm formation was observed at constant dilution rates that were far in excess of the culture maximum growth rate. Baltzis and Fredrickson [17] extend the THM to competition between two different microbial populations for one limiting substrate where only one population forms an attached monolayer (not a strict biofilm). Bryers [18] has in a theoretical paper presented a general mixed culture growth model of a biofilm in a chemostat but no stability analysis of resultant steady-states were made. Kessel et al. [19] presents a elegant mathematical simulation of a mixed-culture biofilm which predicts both spatial and temporal changes as the biofilm developes in a reactor operated at dilution rates well past wash-out.

3 Mathematical rationale

For modelling sake, the biofilm is treated here as a completely mixed continuum. Concentrations of biofilm microorganisms are essentially biofilm-volume-distributed values since a microorganism's location within the biofilm is ignored. This simple approach for mixed culture biofilm development suffices for microorganisms with similar growth rates. For situations where the turnover rates of individual species are markedly different (i.e., heterotropic vs. autotrophic bacteria), spatial distributions can be significant; the reader is directed elsewhere for such models of competition within growing biofilms [19].

Biofilm accumulation is based upon the scenario proposed by Characklis and co-workers [14–16]. A general mixed culture biofilm formation model has been discussed elsewhere [18]. Therefore, only a binary culture model (BCM) will be developed here based upon the following assumptions:

1. The reactor is operated in the continuous flow mode and is completely mixed with a volume V and an internal surface area A.

2. Biomass concentration of the suspended microorganisms is denoted C_j with $j = a, b$.

3. Each suspended microorganism attaches to some extent. Biomass areal concentration of each attached microbe is denoted as $B_j = M_x/A$ with $j = a, b$.

4. Accumulation of each attached microbial species is the sum of three individual rate processes: cellular deposition rate R_j^D, growth rate of attached microbes R_j^G and a fraction f_j of the total biofilm removal rate R^R.

5. Non-viable biofilm material arising from extracellular polymer production or cell lysis is not modelled here. Consequently, the total biofilm areal density M is the sum of the areal concentrations of all attached microorganisms. Bakke et al. [20] does present structured mass balances for both intra- and extracellular carbon in biofilms growing in pure culture chemostats.

6. The fraction f_j is assumed without verification to be equal to the weight fraction of microbe j in the biofilm – i.e., $f_j = B_j/M$. Due to assumption 5, $\sum_{j=1}^{n} f_j = 1.0$.

7. Nutrient feed to the reactor is assumed sterile.

8. Both suspended and attachment mixed cultures grow on a single growth limiting substrate S. Suspended culture growth rates are considered to follow Monod-like expressions of S, – i.e.,

$$\mu_j C_j = \mu_j^* S C_j/(K_j + S)\,. \tag{6}$$

Attached microbial growth rates are identical Monod-like expressions, only replacing suspended with attached microbial concentrations. Biofilm growth rate expressions could also incorporate an effectiveness factor η to account for possible mass transfer resistance to S – i.e.,

$$R_j^g = \eta \mu_j B_j = \eta \mu_j^* S B_j/(K_j + S)\,. \tag{7}$$

External mass transfer resistances are considered here to be negligible in most well-stirred fermenters. Regarding internal mass transfer resistances, Pitcher [21] describes one such effectiveness factor η for Monod kinetics,

$$\eta = \tanh \theta_p/\theta_p\,, \tag{8}$$

where the modified Thiele modulus θ_p can be adapted to biofilm terms – i.e.,

$$\theta_p = \frac{\varphi\left[(L^2/K_s D_e)\sum_{j=1}^{n}(\mu_j B_j/Y_j)\right]^{0.5}}{(1+\varphi)\,[2\varphi - 2\ln_e(1+\varphi)]^{0.5}}\,, \tag{9}$$

where L is the biofilm thickness defined as M/ϱ, ϱ is the biofilm volume density, Y_j is the attached microorganism yield coefficient M_x/M_s, D_e = effective diffusivity of S in the biofilm and φ is defined as S/K_s.

9. Biofilm removal is assumed to be due to prevailing shear stresses in the reactor which are considered constant for this paper. Thus, the rate of biofilm removal is assumed a function of only the total amount of biofilm mass. Trulear and Characklis [15] suggest the following empirical expression for biofilm removal rate,

$$R^R = k^R M^2\,, \tag{10}$$

where k^R is the maximum biofilm removal rate at the maximum attainable biofilm concentration.

10. Cellular deposition rates are assumed proportional to the concentration of specific microorganism in the liquid phase. Examination of data suggests the maximum surface coverage possible by deposition only is 1–3% of the total surface area. Cellular deposition, according to Bryers [22], can be expressed as,

$$R_j^D = k_j^D C_j\,, \tag{11}$$

where k_j^D, the deposition rate, is constant for the jth cell.

Given the above assumptions, the following equations describe binary culture biofilm formation in a chemostat:

Biofilm B_a accumulation equation:

$$\mathrm{d}B_a/\mathrm{d}t = R_a^D C_a + \eta \mu_a B_a - k_a^R B_a^2\,. \tag{12}$$

Biofilm B_b accumulation equation:

$$\mathrm{d}B_b/\mathrm{d}t = R_b^D C_b + \eta \mu_b B_b - k_b^R B_b^2\,. \tag{13}$$

Suspended cell balance, C_a:

$$\mathrm{d}C_a/\mathrm{d}t = -D C_a - R_a^D C_a + \mu_a C_a + k_a^R B_a^2 A/V\,. \tag{14}$$

Suspended cell balance, C_b:

$$\mathrm{d}C_b/\mathrm{d}t = -D C_b - R_b^D C_b + \mu_b C_b + k_b^R B_b^2 A/V\,. \tag{15}$$

Substrate balance, S:

$$\mathrm{d}S/\mathrm{d}t = D(S^0 - S) - [(\mu_a C_a + \eta \mu_a B_a A/V)/Y_a] - [(\mu_b C_b + \eta \mu_b B_b A/V)/Y_b]\,. \tag{16}$$

3.1 Stability analysis

First, the situation described by Eqs. (12)–(16) can be reduced to one of smaller dimensions. Multiplying Eq. (14) by Y_a^{-1}, Eq. (15) by Y_b^{-1}, Eq. (12) by $A/(VY_a)$, Eq. (13) by $A/(VY_b)$ and then adding all resultant equations to Eq. (16), one can see that the system, except for initial times, is very close to the steady-state hyperplane:

$$S = S^0 - C_a/Y_a - C_b/Y_b\,, \tag{17}$$

which can be employed instead of the differential equation for S in the stability analysis around the system singular points.

For small perturbations about any steady-state, let $\Omega_i = C_i - \tilde{C}_i$ and $\xi_i = B_i - \tilde{B}_i$ where $i = a, b$ and $\tilde{C}_i$ and $\tilde{B}_i$ are the steady-state suspended and attached microbial concentrations at a certain set of conditions. Linearizing Eqs. (12)–(16) results in the following:

$$\frac{\mathrm{d}}{\mathrm{d}t}\begin{bmatrix}\Omega_a\\ \xi_a\\ \Omega_b\\ \xi_b\end{bmatrix} = \begin{bmatrix}(\mu_a - D - R_a^D - \mu_a' \tilde{C}_a/Y_a) & (2k_a^R \tilde{B} A V) & 0 & 0\\ (R_a^D V/A - \eta \mu_a' \tilde{B}_a/Y_a) & (\eta \mu_a - 2k_a^R \tilde{B}_a) & 0 & 0\\ 0 & 0 & (\mu_b - D - R_b^D - \mu_b' \tilde{C}_b/Y_b) & (2k_b^R \tilde{B}_b A/V)\\ 0 & 0 & (R_b^D V/A - \eta \mu_b' \tilde{B}_b/Y_b) & (\eta \mu_b - 2k_b^R \tilde{B}_b)\end{bmatrix}\begin{bmatrix}\Omega_a\\ \xi_a\\ \Omega_b\\ \xi_b\end{bmatrix}. \tag{18}$$

The stability analysis of any steady-state can be now be broken into the examination of the eigenvalues of the two submatrices, one for microbe a and one for microbe b. Reviewing the rules of matrix algebra, the characteristic equation for the population a submatrix, for example, is

$$\lambda^2 - (\mathrm{TR}\,\mathbf{A})\,\lambda + (\mathrm{DET}\,\mathbf{A}) = 0\,, \tag{19}$$

where

$$\mathrm{TR}\,\mathbf{A} = \text{trace of } \mathbf{A} = [(\mu_a - D - R_a^D - \mu_a' \tilde{C}_a/Y_a) + (\eta \mu_a - 2k_a^R \tilde{B}_a)]$$

and

$$\mathrm{DET}\,\mathbf{A} = \text{determinant of } \mathbf{A} = [(\mu_a - D - R_a^D - \mu_a' \tilde{C}_a/Y_a) \cdot (\eta \mu_a - 2k_a^R \tilde{B}_a) - (2k_a^R \tilde{B}_a A/V)(R_a^D V/A - \eta \mu_a' \tilde{B}_a/Y_a)]\,.$$

(λ = eigenvalues to submatrix $\mathbf{A}$, $\mu_a' = \mathrm{d}[\mu_a(S)]/\mathrm{d}S$).

The linearized system for population A is said to be asymptotically stable if and only if,

$$(\mathrm{TR}\,\mathbf{A}/2)^2 \geqq \mathrm{DET}\,\mathbf{A} \geqq 0 \tag{20}$$

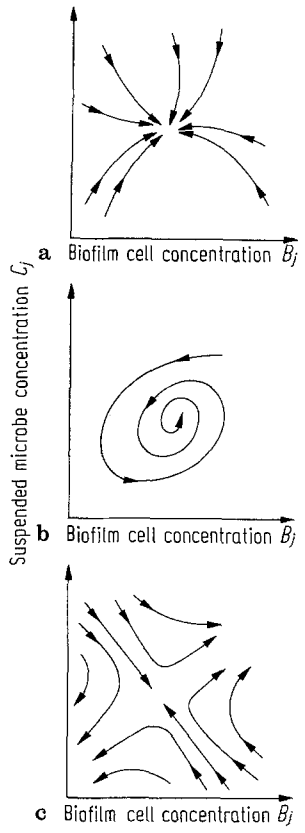

Fig. 1 a – c. Examples of steady-state stability situations

Table 1. Model parameters used in binary culture simulations

Parameters common to all simulations	
A (cm^2)	= 1000.0
V (cm^3)	= 1000.0
k^R (h^{-1})	= 0.6
$K_a = K_b$ (mg$_s$/l)	= 10.0
S^0 (mg$_s$/l)	= 500.0
Specific parameters	
μ_a^* (h^{-1})	= 0.60
μ_b^* (h^{-1})	= 0.50
Y_a (mg$_x$/mg$_s$)	= 0.30
R_a^D (mg/(cm^2 · h))	= 3.0×10^{-6}
R_b^D (mg/(cm^2 · h))	= 3.0×10^{-5} (Case I); 3.0×10^{-3} (Case II)
Batch initial conditions	
$S(0) = 3000.0$ mg$_s$/l, $C_{a,b}(0) = 5.0$ mg$_x$/l, and $B_{a,b}(0) = 0.0$ mg$_x$/cm^2	

then both eigenvalues are real with the same sign and the steady-state in question is called a *node* (illustrated in Fig. 1 a). If the DET **A** is negative, there is one positive and one negative eigenvalue then the steady-state is called a *saddle point* (Fig. 1 b) which is always an unstable condition. Should $(4 \cdot \text{DET A}) \geqq (\text{TR A})^2$, complex eigenvalues occur and the steady-state is called a *focus* (Fig. 1 c). A similar criteria for population b exists based upon submatrix **B**, Eq. (18).

Results of a stability analysis of the steady-states predicted by the BCM simulations for Case I and Case II conditions are presented in the next section.

4 Results

Illustration of biofilm effects on a mixed culture will be considered here only for a simple binary culture, with both microbes competing, attached and suspended, for a single substrate. Growth kinetics for each microbe are such that ($\mu_a^* > \mu_b^*$, $K_a = K_b$) and are selected since, under ideal circumstances, microbe a or b will not co-exist in a chemostat. Other mixed culture scenarios are possible based on either different growth kinetics or on the specific microbial interactions involved.

Two hypothetical cases based upon the above kinetics are treated with the binary culture model (BCM). In both cases the deposition rate of the slower growing microbe b is greater than for microbe a; in Case I $R_b^D = 10 \cdot R_a^D$ and in Case II $R_b^D = 1000 \cdot R_a^D$. Other model parameters used in the BCM simulations are given in Table 1. Biofilm density is set equal to 50 mg$_x$/cm^3 which has the effect of cultivating "computer-wise" a thin but reactive biofilm. At this specific density, a biofilm would have to exceed ≈ 100 μm before internal mass transfer resistance become significant. In the following hypothetical situations, biofilm thicknesses never exceed 100 μm, thus tacitly ignoring internal mass transfer effects.

Both hypothetical cases I and II are initiated as batch reactor simulations with the batch initial conditions given in Table 1. After eight hours simulated batch operation, continuous flow is initiated by setting $D = 0.1$ h^{-1}. The dilution rate is then incrementally increased from 0.1 to 6.0 h^{-1} (Case I); 3.0 h^{-1} for Case II modelling a typical chemostat experiment. Elapsed time between D shifts is the following: 30 hours for $D = 0.1$ h^{-1}, 20 hours for $D = 0.2-0.9$ h^{-1}, and 10 hours for $D = 1.0-3.0$ h^{-1}. Equations comprising the BCM required numerical solution using a dynamic simulator computer package called MIMIC [23].

4.1 BCM simulations: Case I

This case simulates microbe a growing faster than microbe b, both in suspension and in a biofilm but microbe b has a ten times greater deposition rate. Deposition is modelled here as microbe transport to, plus attachment at, the reactor surface. Therefore, a higher deposition rate for one species may arise from that species' greater ability to produce either extracellular polymers or holdfast structures.

Steady-state effluent substrate, suspended cell concentrations ($C_{a,b}$), biofilm composition ($B_{a,b}$), and apparent

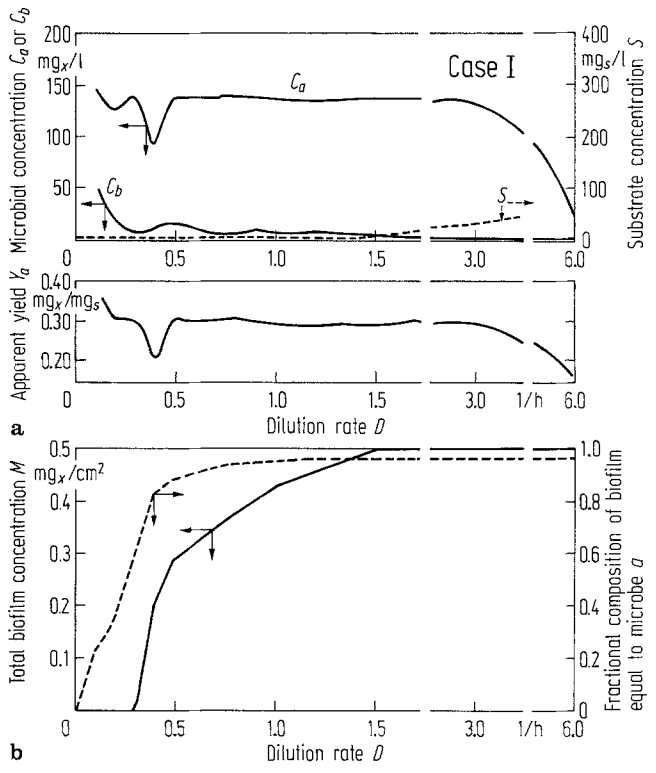

Fig. 2. a Predictions for Case I conditions (see Table 1) for steady-state effluent concentrations of both microbes *a* and *b* plus limiting substrate and apparent yield values Y_a calculated using equation (21). **b** Predictions for total biofilm concentration (M) and the fraction of microbe *a* in the biofilm (f_a) under Case I conditions

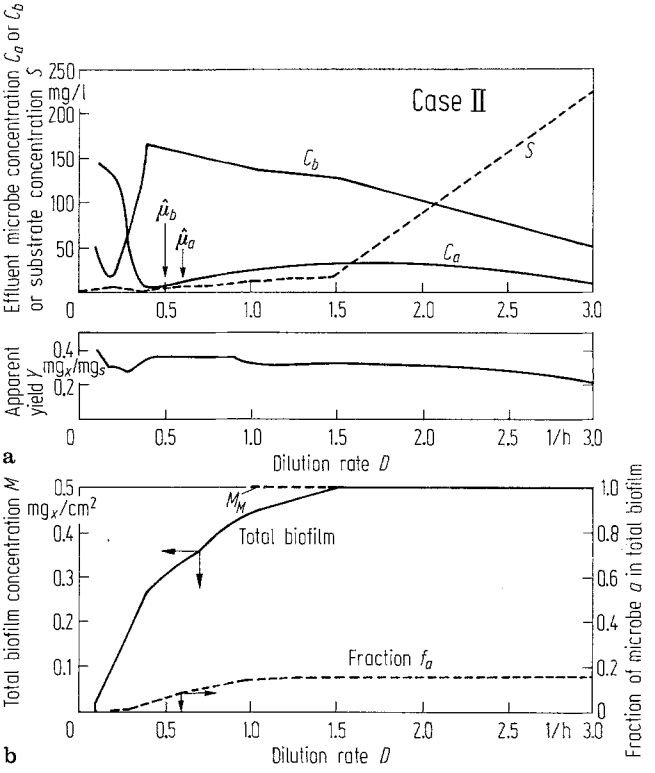

Fig. 3. a Predictions for Case II conditions (see Table 2) for steady-state effluent concentrations of microbes *a* and *b* and the limiting substrate plus apparent yield values Y_a calculated using erroneous equation (21). **b** Predictions for total biofilm concentration (M) and the fraction of microbe *a* in the biofilm (f_a) under Case II conditions

yield values predicted from the BCM for Case I conditions are given in Figs. 2a and 2b.

Microbe *a* is predicted to persist in the reactor until $D = 6.0\,h^{-1}$ (residence time = 0.167 h or ~ 10 min), characteristic for chemostat biofilm formation. Not unexpectedly, microbe *a* dominates the suspended culture, although the BCM also predicts microbe *b* to remain in the reactor until $D = 6.0\,h^{-1}$ but at very low concentrations ($C_a \leqq 3.0\,mg_x/l$). Predicted microbe *a* biofilm concentrations indicate the higher microbe *a* growth rate more than compensates for the ten times greater deposition rate of microbe *b*. At $D = 1.2\,h^{-1}$, microbe *a* comprises ≧ 90% of the biofilm. Apparent yield values (Fig. 2a) vary during D shifts due to changes in culture composition and the wash-out or dilution effect at $D = 0.4\,h^{-1}$ which is muted by increasing biofilm formation. At $D \geqq \mu_a^*$, apparent yield values equal the true stoichiometry for microbe *a* due to its dominance in the biofilm, the origin of all suspended biomass at these dilution rates.

4.2 BCM simulations: Case II

Case II simulates identical conditions to Case I except the deposition rate of microbe *b* is now thousand times that of microbe *a*.

Steady-state effluent substrate concentrations, suspended microbe concentrations ($C_{a,b}$), biofilm composition (M and f_a), and the apparent yield values predicted by the BCM as a function of D are given in Figs. 3a and 3b. Figure 3a again shows both microorganisms to persist in the reactor until a dilution rate of $3.0\,h^{-1}$ (mean residence time = 0.33 h = 20.0 min) due to biofilm formation but, unlike Case I, here microbe *b*, the slowest growing of the two microbes, predominates the culture fluid at $D \geqq 0.3\,h^{-1}$. Although C_a is predicted to persist throughout the simulated experiment, C_a concentrations after $D = 0.3\,h^{-1}$ never exceed $30\,mg_x/l$. Given the advantages of a much higher deposition rate, microbe *b* dominates the early biofilm, not allowing microbe *a* to establish and take advantage of it's higher growth rate.

Transient changes in microbe *a* and *b* concentrations predicted after a shift-up from $D = 0.2 \rightarrow 0.3\,h^{-1}$ (Figs. 4a and 4b) further illustrate the dominance of microbe *b* over microbe *a* due to the higher microbe *b* biofilm concentration. Apparent yield values never equal the true stoichiometry for either species except for conditions between $D = 0.5-0.8\,h^{-1}$, because of the combined influence of both biofilm microorganisms on substrate utilization. Changes in the various process rates at different

Table 2. Summary of stability analysis for populations *a* and *b* under case I conditions

Population *a*						
D (h^{-1})	0.2	0.3	0.4	0.5	1.5	3.0
C_a (mg_x/l)	125.0	140.0	90.0	140.0	140.0	140.0
B_a (mg_x/cm^2)	1.5×10^{-4}	1.5×10^{-3}	0.185	0.27	0.495	0.495
S (mg_s/l)	~1.0	~1.0	~1.0	~1.0	10.0	35.0
TR **A**	−20.8	−23.3	−15.4	−23.8	−8.5	−3.9
DET **A**	−1.11	−1.23	+2.6	+6.4	+2.8	+0.97
[TR **A**/2]^2	+105.4	+153.7	+58.9	+141.7	+18.1	+4.0
4 · DET **A**	−4.4	−4.92	+10.2	+25.4	+11.0	+4.0
Type of steady state	Saddle point	Saddle point	Stable node	Stable node	Stable node	Stable node
Population *b*						
C_b (mg_x/l)	15.0	7.5	10.0	12.5	7.0	2.0
B_b (mg_x/cm^2)	0.149	0.268	0.235	0.18	5×10^{-4}	5×10^{-4}
TR **B**	−2.0	−1.41	−1.77	−2.1	−1.3	−2.2
DET **B**	+0.26	+0.32	+0.37	+0.33	+0.37	−1.0
[TR **B**/2]^2	+1.0	+0.5	+0.8	+1.1	+0.4	+1.3
4 · DET **B**	+1.04	+1.3	+1.48	+1.33	+1.49	−4.1
Type of steady state	Stable node	Stable node	Stable node	Stable node	Saddle point	Saddle point

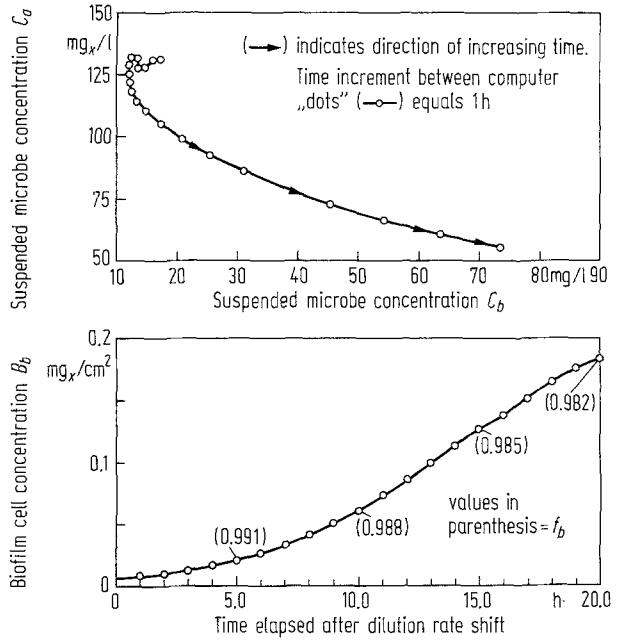

Fig. 4. **a** Transient response of suspended microbes *a* and *b* concentrations and **b** biofilm cell concentrations during a dilution rate shift-up from $D = 0.2 \rightarrow 0.3\ h^{-1}$. (→) indicates in *a* the direction of increasing elapsed time

stages of biofilm development are shown in Fig. 5 which illustrates the dynamics of biofilm formation in a chemostat.

4.3 Stability analysis results

Tables 2 and 3 summarize the calculations of the TR and DET for the two population sub-matrices in Eq. (18). Most steady-states proved to be asymptotically stable nodes. Under Case I conditions, microbe *a* exhibits unstable saddle-point behavior at dilution rates of 0.2 and $0.3\ h^{-1}$ as shown in Fig. 6 for the transient period between $D = 0.2 \rightarrow 0.3\ h^{-1}$. Microbe *b* exhibits similar unstable saddle points at $D = 1.5-3.0\ h^{-1}$. For Case II conditions, microbe *a* steady-states exhibit unstable saddle point behavior at all dilution rates while microbe *b* steady-states are stable nodes at all dilution rates save one, $D = 0.2\ h^{-1}$. Unstable saddle point behavior under the two Cases corresponds to conditions of very minute concentrations of the particular population in the biofilm.

5 Model limitations

Mass transfer and endogenous decay, two processes pertinent to biofilms, were either implicitly or explicitly ignored in the examples above. The impact of neglecting these fundamental processes on the above results is not trivial and warrants discussion.

Under the simulation conditions above, internal mass transfer effects, although incorporated in the model (via η, the effectiveness factor), were tacitly ignored. External mass transfer resistances were explicitly ignored for the well-mixed fermenters considered. However, in certain situations (e.g., plug flow reactors, slow moving streams or quiescent aquatic systems) mass transfer effects could be significant. Under biofilm parameters (e.g., L, ϱ, μ^*, D_e, K) different from those used here, the modified Thiele modulus, θ_p could be such that the effectiveness factor $\eta \leqq 1.0$.

Table 3. Summary of stability analysis for populations *a* and *b* under Case II conditions

Population *a*						
D (h^{-1})	0.2	0.3	0.4	0.5	1.5	3.0
C_a (mg_x/l)	135.0	60.0	5.0	5.0	25.0	5.0
B_a (mg_x/cm^2)	1.5×10^{-4}	1.9×10^{-3}	0.01	0.015	0.075	0.075
S (mg_s/l)	3.0	~1.0	~0.5	~2.0	10.0	230.0
TR **A**	−15.9	−10.1	−1.26	−1.01	−2.2	−1.8
DET **A**	−2.22	−5.3	−0.02	−8.9	−7.1	−1.4
[TR **A**/2]^2	+63.1	+25.4	+0.40	+0.25	+1.20	+0.9
4 · DET **A**	−8.8	−21.1	−0.08	−35.9	−28.5	−5.5
Type of steady state	Saddle point	Saddle point	Saddle point	Saddle point	Saddle point	Saddle point
Population *b*						
C_b (mg_x/l)	20.0	60.5	165.0	160.0	130.0	65.0
B_b (mg_x/cm^2)	0.099	0.188	0.274	0.295	0.492	0.493
TR **B**	−1.73	−7.5	−22.1	−10.8	−3.0	−6.6
DET **B**	−2.98	+1.26	+6.55	+2.7	+0.81	+0.58
[TR **B**/2]^2	+0.75	+14.1	+121.7	+29.1	+2.3	+10.8
4 · DET **B**	−11.9	+5.0	+26.0	+10.83	+3.2	+2.3
Type of steady state	Saddle point	Stable node	Stable node	Stable node	Stable node	Stable node

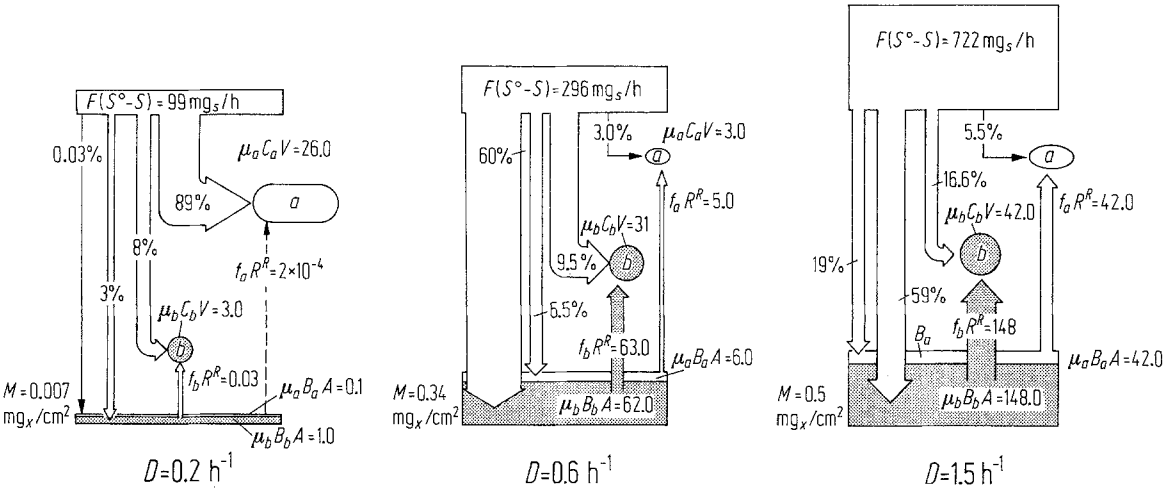

Fig. 5. Process dynamics predicted at three different stages of biofilm formation in Case II. Unless otherwise annotated, all numerical values represent biomass production rates and have units (mg_x/h). Note at $D = 1.5\,h^{-1}$ biofilm is constant at $M = 0.5\,mg_x/cm^2$ and biofilm growth rates for both microbes *a* and *b* equal their respective biofilm removal rates

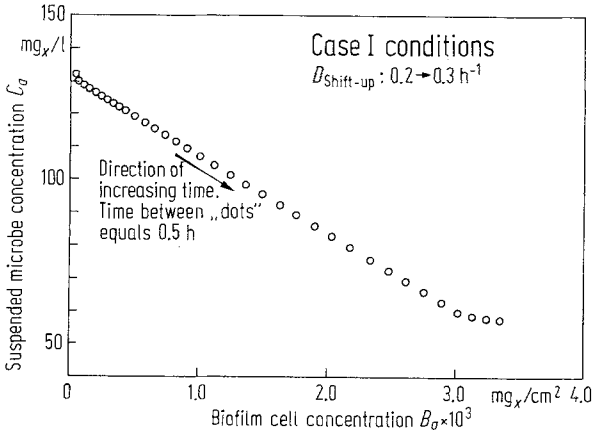

Fig. 6. Illustration of saddle point behavior for population *a* after a dilution rate shift-up from $D = 0.2 \rightarrow 0.3\,h^{-1}$ under Case II conditions

What impact would either a finite mass transfer resistance (external or internal) or a significant endogenous decay have on the results above? Several mechanisms could, alone or in combination, control the overall biofilm substrate removal rate; they are: 1) substrate mass transport to the biofilm, 2) substrate transport within the biofilm along with 3) simultaneous biological reaction. Substrate mass transfer within the biofilm has been traditionally modelled with *molecular diffusion* only, but recent results [24] indicate *convective transport* within a biofilm can occur; however, such a novel transport mechanism will not be considered in this discussion. Only the effects of finite molecular mass transfer will be discussed for pure and mixed culture cases.

For pure culture situations, finite internal or external mass transfer resistances would effectively reduce the overall substrate removal rate of the biofilm at a certain substrate concentration. This would, in turn, reduce the biofilm development rate and the portion of the suspended biomass in the chemostat that originates as biofilm. Generally speaking, external mass transfer resistances would reduce the deviation from ideal chemostat theory created by a biofilm's presence but would also reduce the maximum overall substrate removal rate. Specifically, for first order intrinsic biological reactions (i.e., $S \ll K_s$), external mass transfer does not change the apparent order of the overall substrate removal rate since both transport and reaction are first order processes; only the apparent rate constant value is changed. For zero order kinetics (i.e., $K_s \ll S$), the observed rate is not influenced by external mass transfer.

Numerous articles exist describing the effects of internal mass transfer on biofilm substrate removal rates [13]. For the pure culture case, where microorganisms are uniformily distributed throughout the biofilm, internal mass transfer effectively reduces the amount of biofilm entrained into the liquid. As with external mass transfer, the general impact of internal mass transfer is to reduce the deviation, caused by biofilms, from ideal chemostat behavior. Note external mass transfer resistances are subject to change by engineering factors (e.g., fluid velocity) while internal mass transfer is a function of the physical and biological properties of the biofilm.

Little is known about the processes of microbial death, endogenous decay, lysis, and exopolymer degradation within a biofilm. Generally, all such processes will detract from the rate of biofilm development and will decrease the apparent efficiency of substrate conversion to cellular biomass. One must also be aware that endogenous respiration, the continued uptake of electron acceptor under electron donor starvation, is intimately tied to finite internal mass transfer limitations. As resistances increase, lower portions of the biofilm will not receive substrate, causing endogenous processes to prevail at these lower depths. Such situations could lead to the massive sloughing of biofilm so commonly reported in practice [25].

Mass transfer effects on mixed culture biofilms is a far more complex issue and one that if treated rigorously, would require a more complex model than presented here. Such models have only just appeared in the literature [19, 26]. Conceptually, the model derived here assumes the individual populations are uniformily distributed throughout the biofilm volume and is adequate for mixed culture systems where the microbial turnover rates of each species on the same limiting substrate do not differ dramatically. This naïve approach does ignore those situations where two or more groups of microorganisms, mediating different biological reactions at markedly different rates, compete for one or more limiting substrates. For example, where carbon removal and nitrification are combined in a wastewater treatment fixed-film reactor, heterotrophic bacteria oxidizing organic carbon grow at markedly higher rates than the autotrophic nitrifiers oxidizing NH_4 to NO_2 then to NO_3. Finite mass transfer resistances, could foster a situation where local bacterial turnover rates differ drastically between species. If the total biofilm density remains constant during growth, then the different microbial turnover rates would create *spatial* profiles of each group in the biofilm. In such cases, the net biofilm accumulation rate is an integral value of the species local net biomass production rates. Biomass removal from the biofilm would be dominated by the faster growing organism that is likely to inhabit the upper layers of the biofilm. The model derived here does not pretend such sophistication and for this article such a complex model is not required.

6 Concluding remarks

The dynamic model developed here extends previous steady-state constant biofilm models by simulating not only the extension of wash-out brought about by the biofilm's presence, but also variable yield trends more accurately. The model consists of simple material balances that can be easily modified to simulate a) various mixed culture interactions, b) different suspended growth dependencies on one or more substrates, and c) various biofilm processes neglected here (e.g., internal mass transfer and endogenous decay).

Implications of the above analysis of biofilm formation in a chemostat, subject to the limitations above, are the following:

1. Biofilm formation will bias not only μ^* values estimated from wash-out experiments but can also, if not considered, contribute to erroneous estimates of cellular stoichiometry. Efforts to either minimize biofilm formation or, during an experiment, measure biofilm formation for use in appropriate material balances are urged.

2. Estimates of stoichiometry in either pure or mixed cultures, using Eq. (21)

$$Y_{obs} = M/(S^0 - S)\,, \tag{21}$$

where Y_{obs} is the overall yield, are wrong if biofilm formation occurs. This equation ignores that part of the substrate used in biofilm growth, thus underestimating the true stoichiometry.

3. Effluent suspended biomass in a chemostat experiencing biofilm formation arises due to suspended growth and biofilm removal processes. As dilution rate approaches and exceeds μ^* that portion of the suspended biomass due to suspended growth decreases. Although well past μ^*, suspended biomass from the biofilm can actually utilize substrate at a significant rate.

Note the tacit problem implied above with regard to data comparison between experiments in different systems. Biofilm removal rates are highly dependent upon prevailing shear stresses. Consequently, two identical cultures, grown under identical nutrient conditions but different hydrodynamics (i.e., impeller speed, number, and location; number of baffles, etc.) could produce different effluent biomass concentrations.

4. Decreasing apparent yield values with decreasing growth rate (or D) may not be due to so-called maintenance requirements, but can as shown here, be attributed to biofilm formation.

5. Successive wash-out of different members of a mixed population will be biased under conditions experiencing biofilm formation. Depending on the cell's ability to remain at a surface and attach, a higher growth rate is not sufficient to insure dominance of one species over another.

6. Model predictions suggest biofilms can be metabolically more active (based upon total substrate uptake) than suspended biomass. Yet, until recently [27], microbial activity in most natural aquatic environments has been assessed by sampling free floating rather than sessile or biofilm entrapped cells. Neglecting adherent biomass may underestimate the capacity of a water system to assimilate a particular load.

7. Stability analysis for the two systems indicate a biofilm stabilizes chemostat operation with regard to mixed culture operation, allowing both populations to persist at a variety of dilution rates in asymptotically stable steady-states. Adhesive or kinetic properties different than those employed here may produce different results.

Acknowledgements

This manuscript was prepared while the author was a research fellow within the Applied Process Biology group of the Schweiz. Eidgenössische Anstalt für Wasserversorgung, Abwasserreinigung, und Gewässerschutz (EAWAG) of the Schweiz. Eidg. Technische Hochschulen (ETH). The author deeply appreciates their support in the preparation of this article. Conversations with Profs. Geoffry Hamer and Gregory Stephanopoulos were invaluable.

References

1. Jost, J. L.; Drake, J. F.; Fredrickson, A. G.; Tsuchiya, H. M.: J. Theor. Biol. 41 (1973) 461
2. Aris, R.; Humphrey, A. E.: Biotechnol. Bioengr. 19 (1977) 1375
3. Yoon, H.; Blanch, H. W.: J. Appl. Chem. Biotechnol. 27 (1977) 260
4. Yoon, H.; Klinzing, G.; Blanch, H. W.: Biotechnol. Bioengr. 19 (1977) 1193
5. Stephanopoulos, G.: A.I.Ch.E.J. 26(5) (1980) 802–816
6. Korn, G. A.; Korn, T. M.: Mathematical handbook for scientists and engineers. New York, N.Y.: McGraw-Hill Book Co. 1961
7. Characklis, W. G.: Biotechnol. Bioengr. 23 (1981) 1923–1960
8. Larsen, D. H.; Dimmick, R. L.: J. Bacteriol. 88 (1964) 1380
9. Munson, R. J.; Bridges, B. A.: J. Gen. Microbiol. 37 (1964) 411
10. Zobell, C. E.: J. Bacteriol. 46 (1943) 39
11. Topiwala, H. H.; Hamer, G.: Biotechnol. Bioengr. 13 (1971) 919
12. Wilkinson, T. G.; Hamer, G.: Biotechnol. Bioengr. 16 (1979) 251
13. Grady, C. P. L.: Fixed-film biological processes. In: Wu, Y. C. et al. (eds.): Proc. of the First Int. Conference, April 20–23. Kings Island, Ohio 1982
14. Bryers, J. D.; Characklis, W. G.: Biotechnol. Bioengr. 24 (1982) 2451–2476
15. Trulear, M. G.; Characklis, W. G.: J. WPCF. 54 (1982) 1288
16. Characklis, W. G.; Cooksey, K. E.: Adv. Appl. Microbiol. 29 (1973) 93
17. Baltzis, B. C.; Fredrickson, A. G.: Biotechnol. Bioengr. 25 (1983) 2419–2439
18. Bryers, J. D.: Biotechnol. Bioengr. 26(8) (1984) 948–958
19. Kessel, J. C.; McCarty, P. L.; Street, P. L.: J. Environ. Engr. ASCE 110(2) (1984) 393–411
20. Bakke, R.; Trulear, M. G.; Robinson, J. A.; Characklis, W. G.: Biotechnol. Bioengr. 26 (1984) 1418–1424
21. Pitcher, W. H.: Catalyst Reviews-Sci. and Eng. 12 (1975) 37
22. Bryers, J. D.: Ph.D. Diss. W. M. Rice University, Houston, Texas 1980
23. MIMIC.: Control Data Corp. Ref. Manual Nr. 44610400. Sunnyvale, California 1968
24. Bryers, J. D.: Unpublished data 1984
25. Howell, J. A.; Atkinson, B.: Water Research 10 (1976) 307
26. Gujer, W.; Wanner, O.: Wat. Sci. Tech. 17 (1984) 27
27. Geesey, G.; Mutch, R.; Costerton, J. W.; Green, R.: Limnolog. Oceanog. 23 (1978) 1214

Received September 24, 1985

J. D. Bryers
Center of Biochemical Engineering
School of Engineering
Duke University
Durham, North Carolina 27706
USA